J|A|C|S ARTICLES

Published on Web 12/15/2010

Reversible Two-Photon Photoswitching and Two-Photon Imaging of Immunofunctionalized Nanoparticles Targeted to Cancer Cells

Ming-Qiang Zhu,*,† Guo-Feng Zhang,† Chong Li,† Matthew P. Aldred,† Emmanuel Chang,‡ Rebekah A. Drezek,*,‡ and Alexander D. Q. Li*,§

Wuhan National Laboratory for Optoelectronics, Huazhong University of Science and Technology, Wuhan 430074, China, Department of Bioengineering, Rice University, Houston, Texas 77005, United States, and Department of Chemistry, Washington State University, Pullman, Washington 99163, United States

Received August 9, 2010; E-mail: mqzhu@mail.hust.edu.cn; drezek@rice.edu; dequan@wsu.edu

Abstract: Both photoswitchable fluorescent nanoparticles and photoactivatable fluorescent proteins have been used for super-resolution far-field imaging on the nanometer scale, but the photoactivating wavelength for such photochemical events generally falls in the near-UV (NUV) region (<420 nm), which is not preferred in cellular imaging. However, using two near-IR (NIR) photons that are lower in energy, we can circumvent such problems and replace NUV single-photon excitations (e.g., 390 nm) with NIR two-photon excitations (e.g., 780 nm). Thus, we have demonstrated that alternating 780 nm NIR two-photon and 488 nm single-photon excitations induces reversible on−off fluorescence switching of immunotargeted nanoparticles in the human breast cancer cell line SK-BR-3. Herein, two-photon absorption not only caused spiropyran−merocyanine photoisomerization within the particles but also imparted red fluorescence. In comparison with single-photon NUV excitations, two-photon NIR laser excitations can potentially reduce absorption-related photodamage to living systems because cellular systems absorb much more weakly in the NIR.

Introduction

Photochromism is a light-induced phenomenon in which chemical species are transformed between two forms that have distinct absorption spectra.[1] In contrast to temperature- and pH-responsive materials,[2,3] photochromic materials require that either their nanoassemblies or their organic molecular groups respond to incident light.[4,5] In the past few decades, interest in gaining insight into the photochromic properties of materials has been rapidly expanding.[6−8] Organic molecular photoswitches, especially spiropyrans (SPs), have been widely utilized in the engineering of photochromic materials, including organic polymers and organic−inorganic hybrid thin films.[9−11] Under NUV irradiation, colorless SPs undergo photoinduced ring-opening reactions, yielding the corresponding isomeric merocyanines (MCs), which absorb strongly in the visible range at 500−600 nm.[6] Back-conversion from MCs to SPs occurs thermally at relatively low rates but is significantly accelerated by visible-light illumination.[12]

Current research interest in SPs has focused mainly on the investigation of the photochromic properties of SPs rather than their fluorescence properties because the fluorescence of SPs is rather weak under "normal" conditions.[12] However, the fluorescence is dramatically amplified when SP molecules are incorporated into the hydrophobic nanocavities of polymers.[13] In such environments, alternating NUV and visible-light exposures cause reversible isomerization between the nonfluorescent spiro- and highly fluorescent mero- forms, turning the fluorescence "on" and "off." This is important in optical molecular bioimaging because the fluorescence of the corresponding photochromic nanoparticles can also be optically switched "on" and "off" under irradiation with NUV or visible light. In comparison with photochromic signals, which depend on color changes, fluorescence detection is generally more sensitive and thus holds great promise for applications in sensors, biolabels, and bioimaging. For example, the applications of photochromic

† Huazhong University of Science and Technology.
‡ Rice University.
§ Washington State University.

(1) *Organic Photochromic and Thermochromic Compounds*; Crano, J. C., Guglielmetti, R. J., Eds.; Plenum Press: New York, 1999.
(2) Zhu, M.-Q.; Wang, L.-Q.; Exarhos, G. J.; Li, A. D. Q. *J. Am. Chem. Soc.* **2004**, *126*, 2656–2657.
(3) Kim, J. H.; Lee, T. R. *Chem. Mater.* **2004**, *16*, 3647–3651.
(4) Medintz, I. L.; Trammell, S. A.; Mattoussi, H.; Mauro, J. M. *J. Am. Chem. Soc.* **2004**, *126*, 30–31.
(5) Zhu, L.; Zhu, M.-Q.; Hurst, J. K.; Li, A. D. Q. *J. Am. Chem. Soc.* **2005**, *127*, 8968–8970.
(6) Berkovic, G.; Krongauz, V.; Weiss, V. *Chem. Rev.* **2000**, *100*, 1741–1754.
(7) Guglielmetti, R. In *Photochromism: Molecules and Systems*, revised ed.; Dürr, H., Bouas-Laurent, H., Eds.; Elsevier: Amsterdam, 2003; pp 855−878.
(8) Irie, M. *Chem. Rev.* **2000**, *100*, 1685–1716.
(9) de Silva, A. P.; Gunaratne, H. Q. N.; Gunnlaugsson, T.; Huxley, A. J. M.; McCoy, C. P.; Rademacher, J. T.; Rice, T. E. *Chem. Rev.* **1997**, *97*, 1515–1566.
(10) Such, G.; Evans, R. A.; Yee, L. H.; Davis, T. P. *J. Macromol. Sci., Polym. Rev.* **2003**, *C43*, 547–579.
(11) Spagnoli, S.; Block, D.; Botzung-Appert, E.; Colombier, I.; Baldeck, P. L.; Ibanez, A.; Corval, A. *J. Phys. Chem. B* **2005**, *109*, 8587–8591.
(12) Minkin, V. I. *Chem. Rev.* **2004**, *104*, 2751–2776.
(13) Zhu, M.-Q.; Zhu, L.; Han, J. J.; Wu, W.; Hurst, J. K.; Li, A. D. Q. *J. Am. Chem. Soc.* **2006**, *128*, 4303–4309.

 © 2011 American Chemical Society

materials with photoswitchable fluorescence (e.g., diarylethenes) have resulted in optical information storage devices, and photoactivatable fluorescent proteins have enabled super-resolution imaging of biological samples.[14−16]

However, a critical issue in using photoswitchable probes to image biological samples remains to be solved. It is well-known that both UV and NUV light, which are high in energy, can induce undesired physiological changes in cells, thus causing photodamage to biological tissues.[17] Therefore, circumventing UV-caused photodamage to living systems has motivated many investigators in both optical information storage and bioimaging. To address this problem, we use two-photon techniques whose wavelengths fall in the NIR optical window, typically between 700 and 1200 nm.[18] Precisely in this optical window, both the absorption and scattering of unstained cells and tissues are relatively low and even negligible at certain wavelengths. This, in turn, results in a deeper light-penetrating depth than visible light.[19] Additionally, NIR two-photon excitations eliminate tissue background from linear fluorescence. In the same context, an additional benefit of two-photon excitation is the reduction in photodamage and hence phototoxicity to living systems outside the focal volume because illumination under two-photon excitations is, in fact, strongly confined to the focal plane.[20] In this report, we demonstrate that alternating 780 nm NIR two-photon and 488 nm single-photon excitations induce reversible "on−off" fluorescence imaging of photoswitchable immunotargeted nanoparticles. To our knowledge, this is the first application of two-photon photoswitching and two-photon fluorescence imaging of photoswitchable polymer nanoparticles immunotargeted to cancer cells.

Experimental Section

Materials. The SP monomer, 5-(1,3-dihydro-3,3-dimethyl-6-nitrospiro[2*H*-1-benzopyran-2,2′-(2*H*)-indole])ethyl acrylate, was synthesized according to the procedures described in the literature.[13] Typically, the SP monomer (3 mg, ∼0.01 mmol) was dissolved in a monomer mixture containing styrene (St, 0.2 mL, Aldrich), butyl acrylate (BA, 0.6 mL, Aldrich) and divinylbenzene (DVB, 0.02 mL, Aldrich) and added into a 38 mL aqueous solution of *N*-isopropylacrylamide (NIPAM, 0.1 g, Aldrich) and Tween 20 (0.1 g, Aldrich). The mixture was deoxygenated by bubbling argon for 20 min and emulsified by continuous stirring for 10 min. Next, the mixture was immersed in a 60 °C oil bath. Finally, the sodium salt of 4,4′-azobis(4-cyanovaleric acid) (ABVA, Aldrich) was added to initiate the polymerization. The polymerization was allowed to continue at 60 °C for 2 h, 80 °C for 2 h, and finally 90 °C for 30 min, after which the mixture was cooled and dialyzed against water for 2 days (fresh water every 12 h) to remove the surfactants and small molecules.

Bioconjugation. The carboxyl groups on the surfaces of the nanoparticles were coupled with antibodies using the 1-ethyl-3,3′-dimethylaminopropyl carbodiimide (EDC, Pierce Co.) and *N*-hydroxysulfosuccinimide (sulfo-NHS, Pierce Co.) method. First, 0.4 mg of EDC (2 mM) and 1.1 mg of sulfo-NHS (5 mM) were dissolved in 0.1 mL of water. The EDC/sulfo-NHS solution was added to 0.1 nmol of nanoparticles in 2 mL of PBS buffer (pH 7.5), and the reaction was allowed to proceed for 20 min at room temperature with continuous gentle mixing. Next, the activating reagents were quenched by addition of 1.4 μL of 2-mercaptoethanol (20 mM), and the quenching reaction was allowed to proceed for 10 min at room temperature. To the same nanoparticles in the 2 mL of PBS buffer, 40 μL of anti-Her2 antibody (1 mg/mL, ∼0.22 nmol) was added. The mixture was incubated at room temperature for 2 h with continuous gentle mixing. Finally, 0.02 mg of PEG-amine 2000 (10 nmol, Nektar) was added to react with excess activated carboxyl groups. The total volume was concentrated to 1 mL by centrifugation using a 100K Nanosep spin-filter device (Pall Life Sciences, Ann Arbor, MI), and the antibody−nanoparticle conjugates were washed over the filter twice with water, after which they were ready for imaging applications.

Imaging. The SK-BR-3 human breast cancer cell line was obtained from American Type Culture Collection (ATCC, Manassas, VA). The cells were cultured (37 °C, 5% CO_2) on glass chamber slides (Nalge Nunc International, Rochester, NY) in McCoy's 5A medium with 10% (v/v) FBS (Invitrogen Corp., Carsbad, CA) overnight. The cells were fixed in 4% paraformaldehyde in PBS. Fixed SK-BR-3 cells were incubated with monoclonal anti-Her2 antibody conjugated to photoswitchable nanoparticle probes for 4 h. The cells were then washed twice with PBS buffer. Imaging examination under UV−vis excitation was conducted with a Zeiss Axiovert 200 fluorescence microscope equipped with a 100× oil aperture objective and an HBO 100 illuminating system. A Nikon color digital camera was used to collect the images. The filter set included 470 ± 40 nm excitation/535 ± 40 nm emission for the green and 400 ± 40 nm excitation/470 nm long-pass emission for the red. The two-photon-excitation fluorescence imaging experiments were conducted on a Zeiss LSM 510 META NLO confocal microscope with a 63× (plan-Apochromat, NA 1.40) oil-immersion objective (Carl Zeiss Microimaging, Inc., Thornwood, New York). The microscope was equipped with an argon ion laser and a Coherent Chameleon Ti:sapphire laser as the two-photon excitation source, which could be tuned over the range 720−950 nm. The Zeiss LSM software was used for the collection and processing of digital images.

Results and Discussion

For most fluorophores, one-photon absorptions occur in the visible spectrum rather than in the NIR region. Thus, although it is a promising energetic wavelength for imaging of biological samples, NIR light is frequently not used because of the lack of such fluorophores. However, two-photon absorption (TPA) using a femtosecond NIR two-photon process makes visible fluorescence possible.[21] The TPA process involves an electronic transition from the ground state to the excited state by simultaneous absorption of two photons. Such a nonlinear process is named two-photon excitation (TPE), in which the single excited electron returns to its ground state, emitting a higher-energy photon. For example, a femtosecond NIR laser from 700 to 1200 nm can excite fluorescent dyes by TPE to impart visible fluorescence. Similarly, TPE can also be used to photoswitch chromophores. For instance, SP nanoparticles, which are usually photoswitched using sub-420 nm light, can also be photoactivated using a sub-840 nm NIR laser in a TPE process (Scheme 1). Under these conditions, TPE not only induces photoisomerization but also imparts red fluorescence when the SP nanoparticles are exposed to a femtosecond NIR laser (e.g., 780 nm).

As shown in Figure 1A, the transmission electron microscopy (TEM) image revealed that the as-synthesized nanoparticles[13]

(14) Irie, M.; Fukaminato, T.; Sasaki, T.; Tamai, N.; Kawai, T. *Nature* **2002**, *420*, 759–760.
(15) Ando, R.; Mizuno, H.; Miyawaki, A. *Science* **2004**, *306*, 1370–1373.
(16) Sauer, M. *Proc. Natl. Acad. Sci. U.S.A.* **2005**, *102*, 9433–9434.
(17) Valeur, B. *Molecular Fluorescence: Principles and Applications*; Wiley-VCH: Weinheim, Germany, 2002.
(18) Williams, R. M.; Zipfel, W. R.; Webb, W. W. *Curr. Opin. Chem. Biol.* **2001**, *5*, 603–608.
(19) Weissleder, R. *Nat. Biotechnol.* **2001**, *19*, 316–317.
(20) So, P. T.; Dong, C. Y.; Master, B. R.; Berland, K. M. *Annu. Rev. Biomed. Eng.* **2000**, *2*, 399–429.
(21) Denk, W.; Strickler, J. H.; Webb, W. W. *Science* **1990**, *248*, 73–76.

Scheme 1. Single-Photon Photoswitching and Fluorescence Excitation Contrasted with Two-Photon Photoswitching and Fluorescence Excitation of SP/MC-Containing Nanoparticles

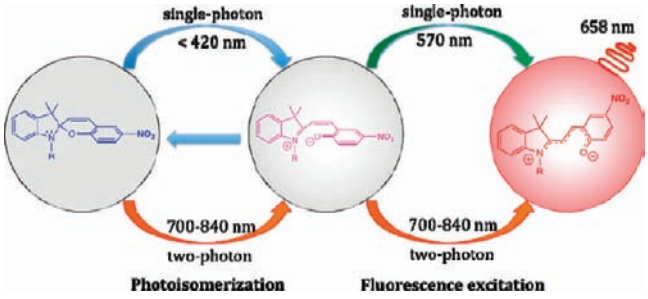

had a mean diameter of ~60 nm. Before and after bioconjugation, TEM revealed little change in particle size. Under alternating 365 and 488 nm light illumination, both the dispersed nanoparticles and their cast thin films featured salient photochromic and photoluminescent behavior (Figure 1B,C). After UV irradiation, SP-containing nanoparticles (SP-nanoparticles) were converted to MC-containing nanoparticles (MC-nanoparticles), thus inducing a new absorption peak that appeared at 588 nm. UV-generated MC-nanoparticles emitted strong red fluorescence at 600−700 nm (excitation wavelength 420 nm). In contrast to MC-nanoparticles, SP-nanoparticles produced no such red fluorescence. The milky-white appearance of dispersed nanoparticles changed to purple after UV irradiation. Reversible photoswitching of patterns was achieved when the nanoparticle dispersion ink was used in dip-pen lithography (Figure 1C). Such patterns could be developed using UV irradiation and then erased using visible light.

Like organic fluorophores, molecular photoswitches (i.e., MC nanoparticles) do suffer from photobleaching, particularly under UV irradiation. Figure 1D shows that the 658 nm fluorescence intensity of MC nanoparticles under 400 nm excitation reaches a maximum in the first 4 min and then gradually decays as time elapses. Initially, UV irradiation results in the SP−MC photoisomerization; the increased amount of MC-particles imparts red fluorescence. Conversely, continuous UV irradiation also causes molecular photobleaching, thus reducing the intensity of the red fluorescence. In the initial stage, MC population augmentation outperforms MC photobleaching, and the red fluorescence therefore intensifies. In the later stage, the fluorescence is attenuated as MC photobleaching becomes predominant and the rapidly switchable SP population is near depletion. The intensity of the red fluorescence is maximized at the equilibrium where the positive SP-to-MC photoisomerization and negative MC photobleaching are balanced. This example illustrates that the effect of photobleaching on photoswitchable fluorophores remains a challenge for further research.

The optical properties of photoswitchable polymer nanoparticles, particularly fluorescent emission, depend dramatically on the monomer feed ratio including BA, St, and SP. When the volumes of both BA and St were 0.4 mL, the optimal photochromism and switched-on photoluminescence of polymer nanoparticles occurred at an SP loading of 3−4 mg (Figure 2A,C). Different polymerization times, such as 1, 4, 8, and 12 h, had little effect on the photochromism and photoswitchable fluorescence. In addition to the minor monomer SP loading, varying the feed ratios of the major monomers BA and St produced nanoparticles having different degrees of photo-

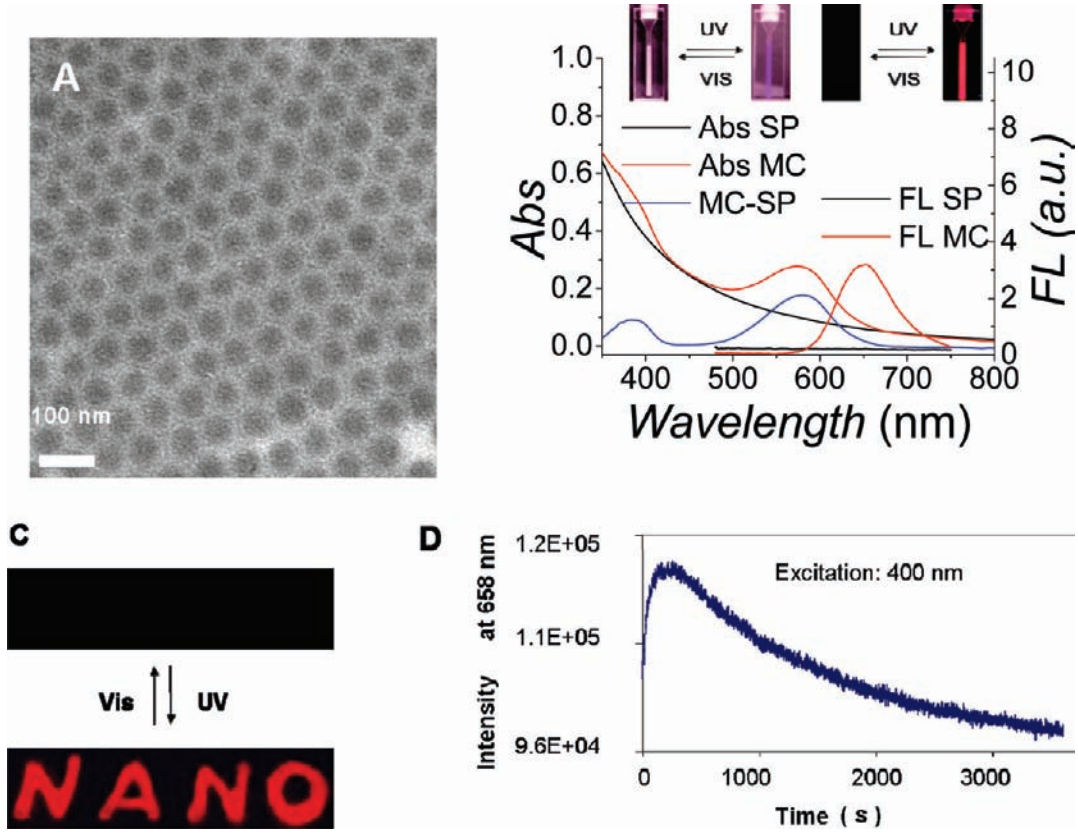

Figure 1. Properties of photoswitchable nanoparticles. (A) Typical TEM image of SP nanoparticles. (B) UV−vis absorption and fluorescence spectra of photoswitchable nanoparticles in water. Inset: (left) photochromism under ambient light; (right) fluorescence photoswitching in the dark. (C) Photoswitchable pattern under alternating UV and visible-light irradiation. (D) Time dependence of the fluorescence intensity of SP nanoparticles under 400 nm excitation. The nanoparticle concentration was 10 nM, and the intensity was acquired every 10 s.

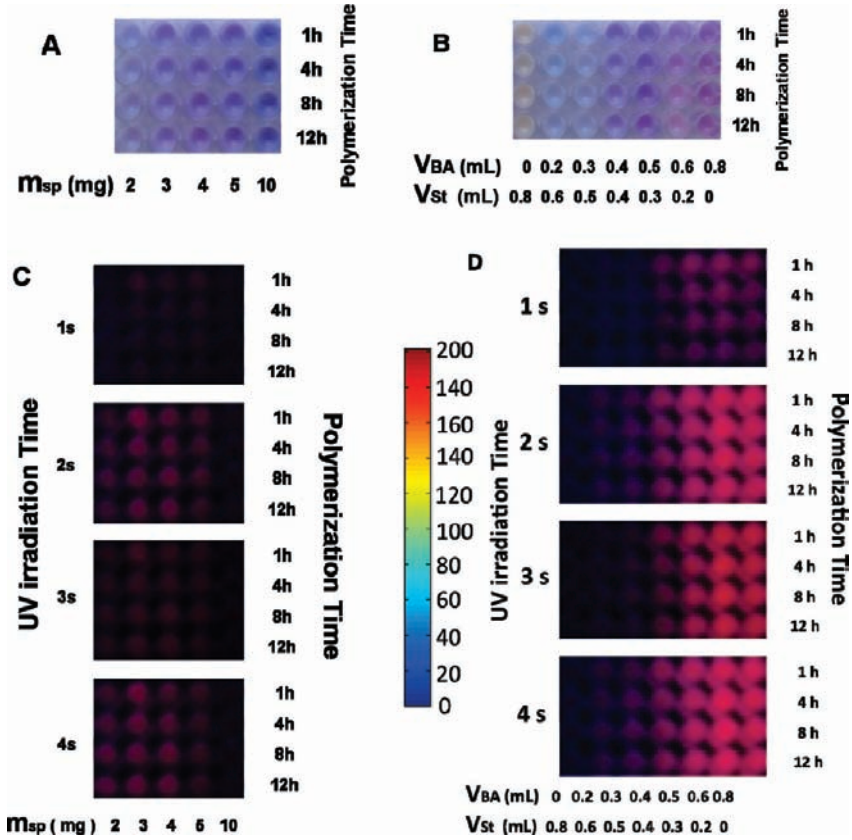

Figure 2. Effects of monomer feed ratio on the reversible photoswitching properties of polymer nanoparticles. (A) UV-induced color patterning of polymer nanoparticles containing different SP monomer contents at various polymerization times with a fixed BA/St feed ratio of 0.4/0.4. (B) UV-induced color patterning of polymer nanoparticles whose BA/St monomer ratios were systematically tuned at various polymerization times (SP content = 4.0 mg). (C) Time-dependent UV-induced fluorescence patterning of polymer nanoparticles containing different SP monomer contents at various polymerization times with a fixed BA/St feed ratio of 0.4/0.4. (D) Time-dependent UV-induced fluorescence patterning of polymer nanoparticles for various BA/St monomer ratios at various polymerization times (SP content = 4.0 mg).

chromism (Figure 2B) and photoswitchable fluorescence (Figure 2D). The optimal BA/St feed ratio was 3:1 (v/v) under these experimental conditions, indicating that the medium in which the latent SP chromophores are located plays a critical role in obtaining the optimal photoswitchable fluorescence (Figure 2D). The comparison between photochromism and photoswitchable fluorescence divulged that red-purple polymer nanoparticles exhibit the strongest red emission, while the emission intensity abates in order for the blue-purple, blue, and white polymer nanoparticles. Therefore, the polymer nanoparticles used for fluorescence imaging in this report had been polymerized for 8 h and synthesized from 3 mg of SP, 0.6 mL of BA, and 0.2 mL of St.

As an alternative to NUV photoswitching, NIR photoswitching followed by illumination with a visible laser is introduced. In comparison with UV light, NIR photons have the potential to cause less photodamage to tissue and cells and induce no single-photon fluorescence in the visible region.[21−23] Thus, fluorescence imaging was carried out on a Zeiss LSM 510 META confocal microscope equipped with an argon ion laser (the visible-light source) and a Coherent Chameleon Ti:Sapphire laser as the two-photon excitation source, which could be tuned from 720 to 950 nm. When the 488 nm laser was used, the fluorescence was switched off (Figure 3A). When the femtosecond NIR laser (780 nm) was used to excite the samples, the red fluorescence was switched on (Figure 3B). Such two-photon forward switching (SP → MC) and single-photon backward switching (MC → SP) are reversible and could be repeated at least 20 cycles without observable diminishment of the signal. These results confirm that the two-photon NIR laser not only activated SP−MC photoisomerization but also acted as the two-photon fluorescence excitation source. Using a multichannel wavelength scanner, we observed no fluorescence under 488 nm laser illumination (Figure 3D,F). Under the 780 nm NIR two-photon laser excitation, however, strong fluorescence from 620 to 700 nm was observed (Figure 3E,F). These results demonstrate that the NIR laser can be used to switch on the fluorescence of SP-nanoparticle thin films, whereas the 488 nm laser may be used to erase the fluorescence patterns.

Although the detailed mechanism of two-photon NIR-induced SP photoisomerization remains unknown to date, we have summarized the observed facts in Table 1. Single-photon NUV photoswitching and two-photon NIR photoswitching produce the same phenomenon (red fluorescence), indicating that both sub-420 nm and NIR (700−840 nm) excitations transform SP-nanoparticles into MC-nanoparticles. SP-nanoparticles do not fluoresce but can be photochemically converted to MC-nanoparticles that emit strong red fluorescence when excited via either visible single-photon processes or NIR two-photon processes. The salient feature is that single-photon fluorescence excitation in the visible region also switches the MC-particles

(22) Larson, D. R.; Zipfel, W. R.; Williams, R. M.; Clark, S. W.; Bruchez, M. P.; Wise, F. W.; Webb, W. W. *Science* **2003**, *300*, 1434–1436.
(23) Albota, M. A.; Xu, C.; Webb, W. W. *Appl. Opt.* **1998**, *37*, 7352–7356.

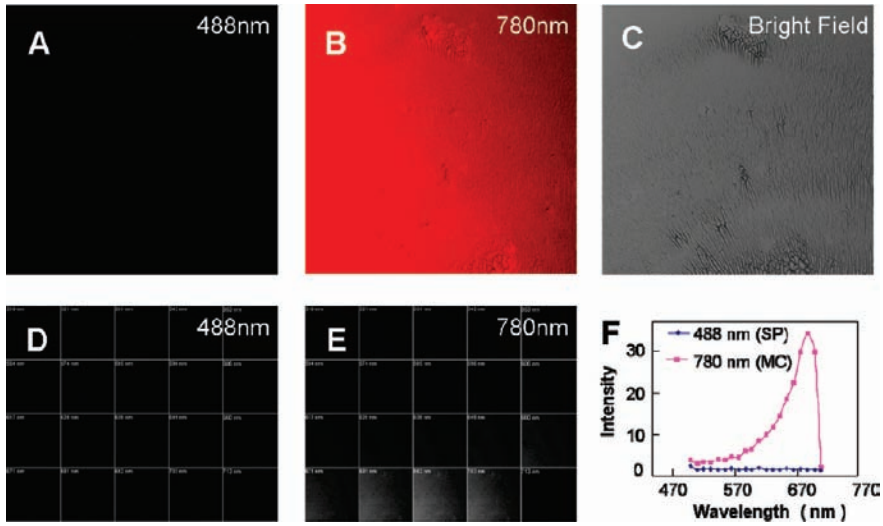

Figure 3. Fluorescence switching using alternating 488 nm single-photon and 780 nm two-photon excitations. (A, B) Fluorescence images of a solution-cast nanoparticle film under 780 nm two-photon and 488 nm one-photon laser excitation, respectively. (C) Bright-field image of the nanoparticle film for comparison and contrast. (D, E) Multichannel wavelength scanning from 560 to 700 nm of the fluorescence emission from the nanoparticle film under the 488 nm blue laser and 780 nm two-photon excitation, respectively. Each small square in **D** and **E** represents fluorescence detection at a particular wavelength. (F) Plots of the scanning results from **D** and **E** against wavelength, yielding the fluorescence spectra of photoswitchable nanoparticles under 488 nm excitation and 780 nm two-photon excitation, respectively.

Table 1. Effects of Various Excitation Wavelengths on SP and MC Nanoparticles

	300−420 nm (one-photon)	420−600 nm (one-photon)	700−840 nm (two-photon)
SP	SP → MC; FL 0 → high	SP; No FL	SP → MC; FL 0 → high
MC	MC; FL high → 0	MC → SP; FL high → 0	MC; steady FL
SP + MC	SP → MC; MC FL	MC → SP; FL high → 0	SP → MC; MC FL

back into nonfluorescent SP-particles, whereas two-photon excitation does not.

The experimental results suggest that excitation into the SP absorption band is necessary to induce photoswitching. The SP absorption maximum occurs at 350 nm, and the absorption band edge extends to 400 nm. Scanning the entire UV−vis spectrum, we found that excitation above 415 ± 5 nm imparted no detectable fluorescence, indicating that SP molecules were not converted into MC dyes. However, excitation below 415 ± 5 nm induced red fluorescence, confirming the photoinduced conversion from SP to MC. Thus, 415 ± 5 nm is the critical wavelength for photoswitching. It is unclear whether photochemical conversion and fluorescence are one-photon processes or two discrete processes. If photochemical conversion and fluorescence are one-photon processes, a single photon excites SP to SP*, which consequently undergoes ring opening and yields excited MC*, which in turn emits red fluorescence (Figure 4). Alternatively, photoexcited SP* relaxes back to the MC ground state via possible intermediates X. The newly formed MC dyes have absorption bands at both 570 and 350 nm and can be excited into higher states and relax back to the first excited state, where they emit red fluorescence (Figure 4). Excitation into virtual states lower than this first excited state does not cause any detectable photoswitching phenomena. Such conclusions are also confirmed by two-photon processes. Only wavelengths lower than 840 nm can cause two-photon excitation and induce SP-to-MC conversion, imparting red fluorescence. No red fluorescence was observed under two-photon excitation above 840 nm. These results indicate that photoexcitation must cause SP to resonance in order to undergo photochemical conversion.

Interestingly, some reports on photoswitchable fluorescent proteins have provided novel concepts and applications in bioimaging.[15,16] As the synthetic photoswitchable probes are similar to fluorescent proteins,[13] the photoswitchable nanoparticles can be equipped with immunoglobulins to gain specific targeting functions. To prevent nonspecific binding, PEG at a density of ∼2400 molecules per particle formed the outer shells with ∼740 carboxylic groups. Thus, the photoswitchable nanoparticles were conjugated with the monoclonal anti-Her2

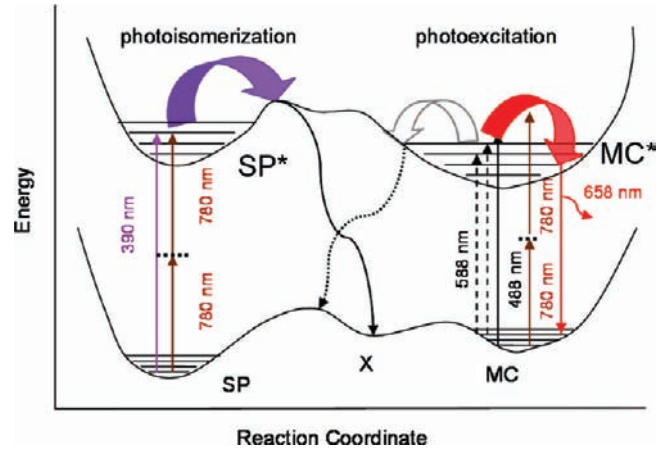

Figure 4. Diagram illustrating both the fluorescence process and the photochemical process. The photochemical process could be strongly coupled to the fluorescence process, and in this situation, one UV photon can induce both photoswitching and red fluorescence. Alternatively, the photochemical process might not be coupled to the fluorescence process. In that case, one UV photon would be required to impart photoswitching and another photon near 350 or 570 nm would be needed to excite the red fluorescence.

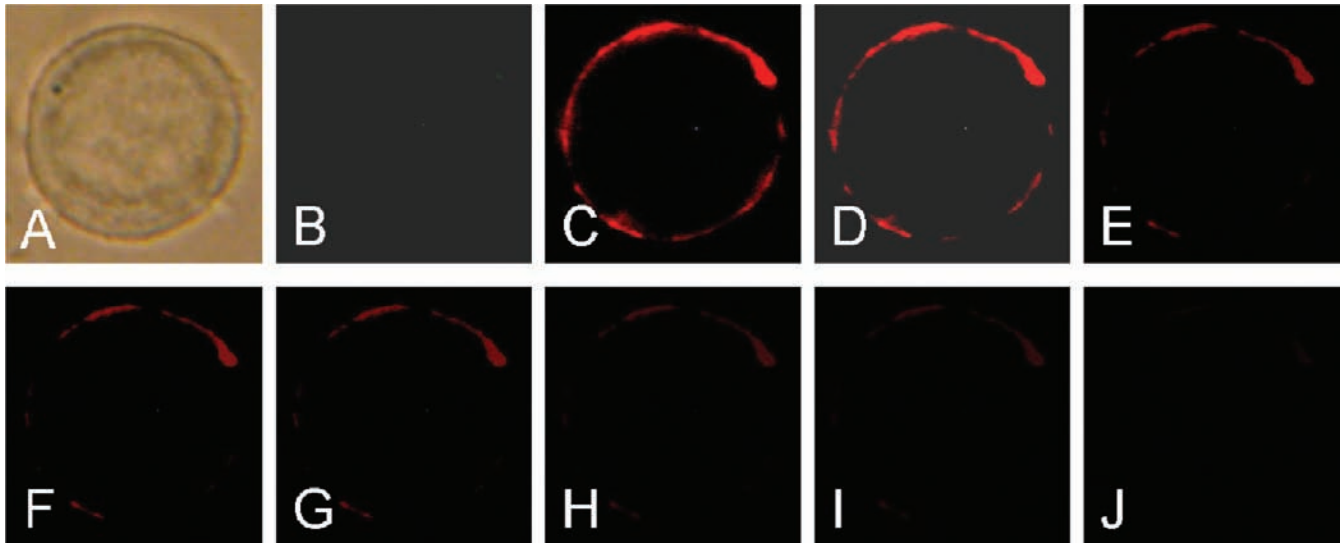

Figure 5. Reversible highlighting of cancer biomarker Her2 on the membrane of SK-BR-3 breast cancer cells using fluorescent photoswitchable probes. (A) Bright-field image displaying the position of the cell. (B) Image of the same cell under 470 nm excitation. (C−J) Images of the same cell under continuous 400 nm excitation recorded at successive 10 s intervals (10, 20, 30, 40, 50, 60, 70, and 80 s, respectively). These results demonstrate that immunofunctionalized photoswitchable particles can be used to target specific membrane receptors such as Her2 on SK-BR-3 cells and that NUV radiation at such power and duration causes relatively quick decay of the red fluorescence. Image sizes: 28 μm × 28 μm.

antibody through the carboxylic groups. The Her2 antibody binds specifically to the Her2 cancer marker overexpressed on the surface of the human breast cancer cell line SK-BR-3. Functionalization of the nanoparticles with Her2 antibodies did not change the emission wavelength and emission intensity of the photoswitchable nanoparticles. Accordingly, photoswitchable nanoparticles conjugated with anti-Her2 antibody were incubated with fixed SK-BR-3 cells. The resulting samples were imaged using a wide-field fluorescence microscope equipped with a color digital camera. As expected, the red fluorescence of targeted SK-BR-3 cells could be reversibly switched between the on and off states depending on the wavelength of excitation light (Figure 5). Similar to organic dyes, the photoswitches in the nanoparticles undergo photobleaching. Repeated exposure to excitation light (HBO 100, Zeiss) eventually caused the red fluorescence to diminish. Figure 5 shows that continuous 400 nm light excitation caused a swift increase in the red emission followed by a gradual decay in intensity. These results demonstrate that (1) polymer nanoparticles can use immunospecificity to target a particular protein and (2) NUV light photobleaches MC dyes under these experimental conditions.

To eliminate the photodamage, phototoxicity, and photobleaching associated with UV irradiation, we used two-photon photoswitching in the NIR to photoswitch SP-particles to MC-particles and two-photon fluorescence to image the switched-on MC-particles specifically bound to Her2 receptors. Figure 6 shows the bright-field image (Figure 6A) and fluorescence images (Figure 6B−F) of SK-BR-3 cells after incubation with the anti-Her2 antibody−nanoparticle conjugates. Under 780 nm two-photon excitation, the membrane Her2 receptors on the SK-BR-3 cells were highlighted with red fluorescence because the photoswitchable nanoparticles had been immunofunctionalized with the targeting anti-Her2 antibody (Figure 6B). Conversely, single-photon laser excitations at 488 nm converted the MC-particles back to SP-particles and switched off the red fluorescence (Figure 6C). Using immunofunctionalized particles and targeted SK-BR-3 cells as the model system, we were able to demonstrate that the red fluorescence could be reversibly switched between the two-photon "on" state and the one-photon "off" state. Such on-and-off cycles regulated by NIR and visible laser illumination could be repeated for at least 20 cycles (Figure 6B−F). In other words, two-photon excitation at 780 nm imparted red fluorescence, while one-photon excitation at 488 nm erased it. Therefore, NIR two-photon photoswitching is a promising alternative to UV irradiation in bioimaging applications using photoactivatable and photoswitchable probes because the issues associated with UV photodamage, phototoxicity, and photobleaching can potentially be alleviated.

Figure 5 illustrates that UV irradiation caused the red fluorescence from the photoswitchable particles immunologically targeted to Her2 of SK-BR-3 cells to decay and mostly disappear after 30 s. For comparison to the one-photon photoswitching and fluorescence excitations, we carried out continuous two-photon illumination of the photoswitchable nanoparticles immunologically bound to SK-BR-3 cells (Figure 7). Instructively, the SK-BR-3 cells were highlighted with red fluorescence and became increasingly brighter as the illumination time elapsed. A possible explanation is that more and more SP-nanoparticles were transformed into MC-nanoparticles under NIR illumination. As the population of the MC-nanoparticles increased with illumination time, the red fluorescence glowed brighter. Therefore, an important conclusion is that under these experimental conditions, photobleaching of MCs under two-photon NIR illumination seemed to be negligible, whereas single-photon UV excitations induced obvious photobleaching.

To compare the relative brightness of MC-nanoparticles and common fluorescent dyes, we measured the two-photon cross section of MC-nanoparticles using rhodamine 6G as a reference.[21−24] The two-photon action cross section (σ_2) of rhodamine 6G in methanol under 780 nm NIR excitation is

(24) *Confocal and Two-Photon Microscopy: Foundations, Applications, and Advances*; Diaspro, A., Ed.; Wiley-Liss: New York, 2002.

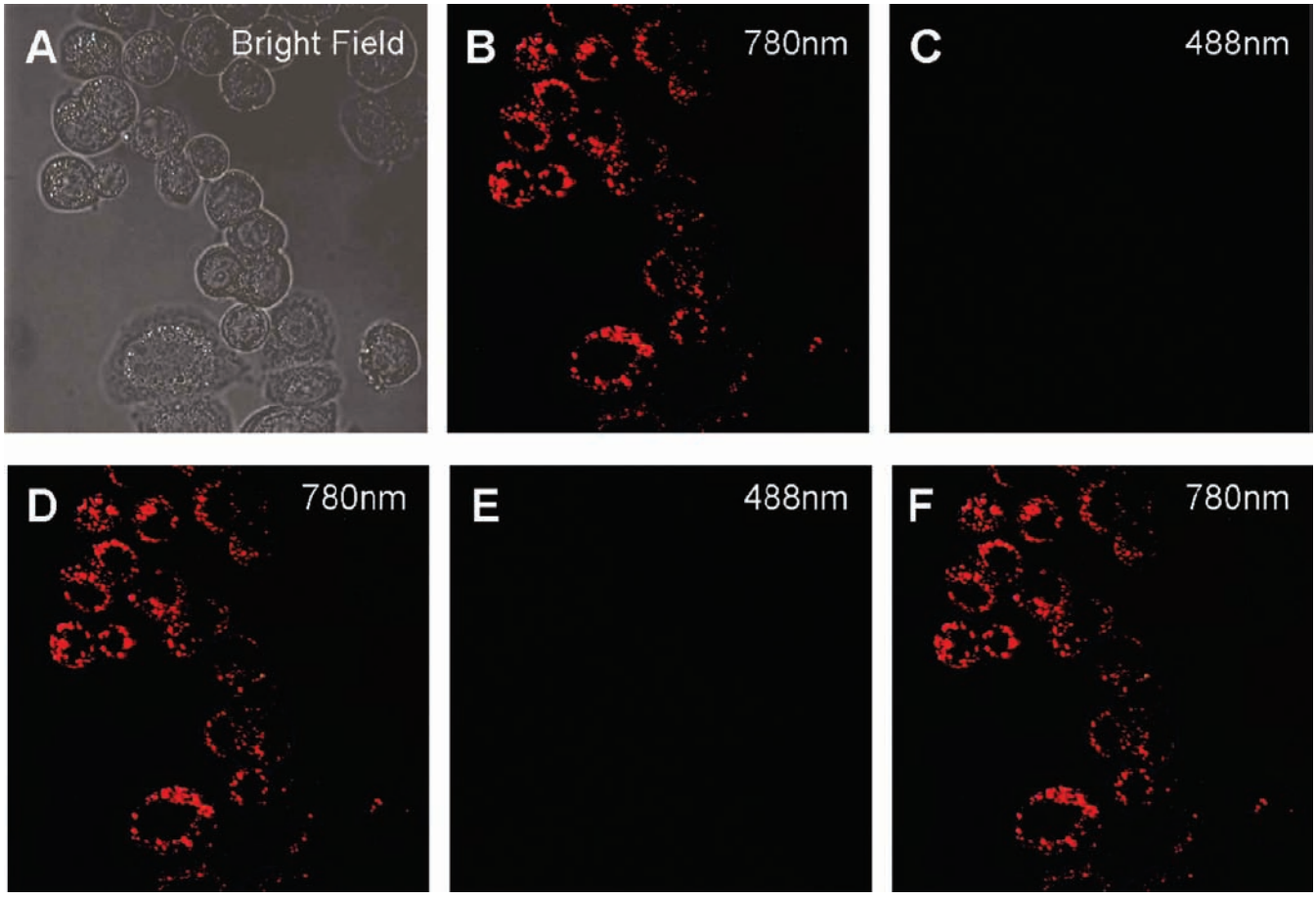

Figure 6. Alternating NIR two-photon and visible single-photon excitations causes photoswitching of the fluorescence imaging of SK-BR-3 cells labeled by anti-Her2 antibody-conjugated photoswitchable nanoparticles. (A) Bright-field images showing the cell locations. (B) Two-photon photoswitching and two-photon imaging at 780 nm of Her2 receptors on the cellular membranes. (C) Single-photon excitation at 488 nm erases the red fluorescence image. (D, F) Repeats of (B). (E) Repeat of (C). Such reversible on−off fluorescence imaging of targeted cells could be repeated at least 20 times. Image sizes 146 μm $\times$ 146 μm.

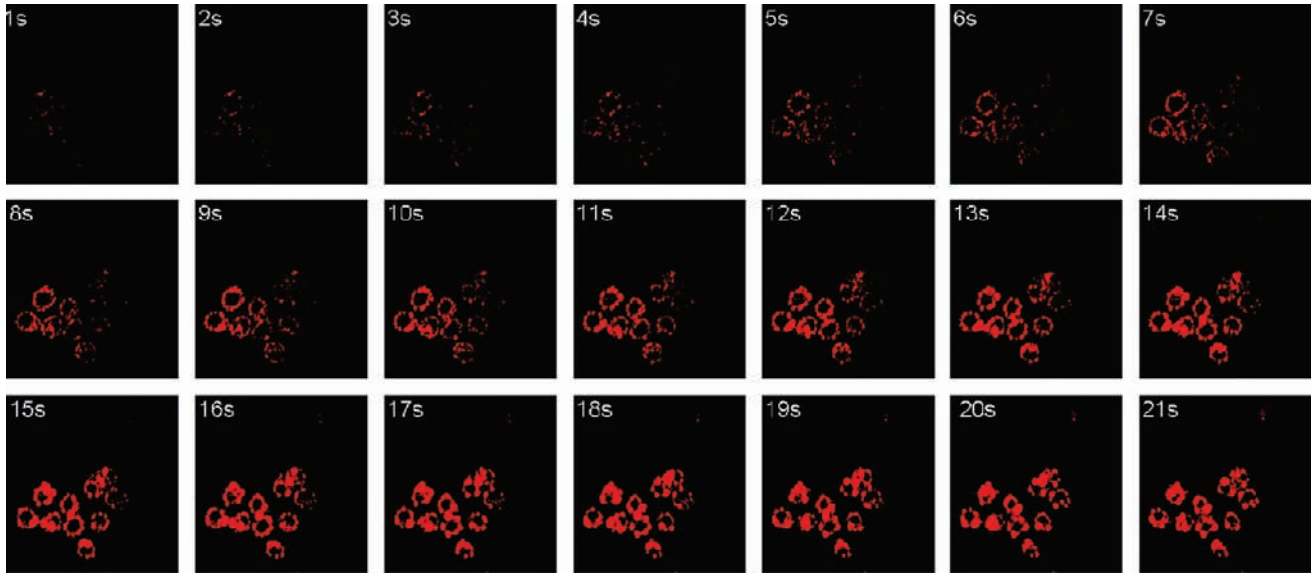

Figure 7. Time dependence of two-photon photoswitching and two-photon fluorescence imaging of anti-Her2 antibody-conjugated photoswitchable nanoparticles anchored on the Her2 receptors of SK-BR-3 cells. Continuous illumination using the NIR laser at 780 nm steadily induced SP-to-MC isomerization and hence intensified the red fluorescence signal. Image sizes: 146 μm $\times$ 146 μm.

30 GM (1 GM = 10^{-50} cm^4 s photon^{-1}). Accordingly, the calculated two-photon action cross section of the MC-nanoparticles in water under 780 nm NIR two-photon excitation was 7 GM, which is comparable to cross sections measured for conventional fluorescent dyes.[21−24] Comparisons between SP/MC-nanoparticles and common organic dyes have also been reported, and the nanoparticles are ~20 times brighter than the dyes.[25] We believe that the SP/MC-

nanoparticles possess promising potential in bioimaging because they not only have two-photon cross sections comparable to those of existing imaging agents but also can be advantageously photoswitched, a distinguishing photochemical property that many existing imaging agents do not have.

Conclusion

In conclusion, this report has demonstrated two-photon photoswitching and two-photon photoluminescence of SP/MC-nanoparticles. Alternating 780 nm NIR and 488 nm visible laser pulses imparted two-photon and one-photon excitations, respectively. The two-photon process photoswitched the SP-particles to MC-particles and also excited the MC-particles to emit red fluorescence. The one-photon process, however, photoswitched the MC-particles back to SP-particles, thus switching off the red fluorescence. Such on−off photoswitching cycles were demonstrated to be reversible in cells and could be repeated up to 20 times. Hence, two-photon excitations of SP nanoparticles are expected to broaden the applications of photoswitchable nanoparticles in advanced bioimaging.

Acknowledgment. We thank Prof. Z. Huang for his kind help with the additional imaging experiments. This work was supported in part by the NSFC (20874025), the Program for New Century Excellent Talents in Universities (NCET-07-0688), the National 973 Project (2007CB310500), the National Science Foundation (NSF) Chemistry Division (CHE-0805547), the Nanoscale Science and Engineering Initiative of NSF (EEC 0118007), and the Department of Defense Congressionally Directed Medical Research Program (DAMD 17-03-1-0384 and DoD CDMRP W81XWH-07-1-0428).

Supporting Information Available: Light scattering data for nanoparticles before and after bioconjugation and the results of control experiments that rule out nonspecific binding between nanoparticles and cells. This material is available free of charge via the Internet at http://pubs.acs.org.

(25) Tian, Z. Y.; Wu, W. W.; Wan, W.; Li, A. D. Q. *J. Am. Chem. Soc.* **2009**, *131*, 4245–4252.

JA106895K